On the three lowest spin states of Na$_{13}^{+}$. Hybrid DFT and Benchmark CASSCF(12,12)+CASPT2 studies

Emiliano Isaías Alanís-Manzano[†,‡] and Alejandro Ramírez-Solís[*,†]

†Depto. de Física, Centro de Investigación en Ciencias-IICBA Universidad Autónoma del Estado de Morelos, Cuernavaca Morelos 62209 México.

‡Current adress: Instituto de Ciencias Físicas, Universidad Nacional Autónoma de México, Cuernavaca Morelos 62210 México.

E-mail: alex@uaem.mx

Abstract

The three lowest spin states (S=0,1,2) of twelve representative Na$_{13}^{+}$ isomers have been studied using both, KS-DFT via three hybrid density functionals, and benchmark multireference CASSCF and CASPT2 methods with a couple of Dunning's correlation consistent basis sets. CASSCF(12,12) geometry optimizations were carried out. Since 12 electrons in 12 active orbitals span the chemically-significant complete valence space, the results of the present study provide benchmarks for Na$_{13}^{+}$. The CASPT2(12,12)/cc-pVTZ* lowest energy structures are three nearly degenerate singlets (S=0): an isomer formed from two pentagonal bipyramids fused together (PBPb), a capped centered-squared antiprism [CSAP-(1,3)] and an optimum tetrahedral OPTET(II) structure, the last two lying 0.88 and 1.63 kcal/mol above the first, respectively. The lowest triplet (S=1) and quintet (S=2) states lie 4.33 and 3.77 kcal/mol above the singlet global minimum, respectively. The latter is a deformed icosahedron while the former

1

is a CSAP-(1,3). The flatness of the potential energy surface of this cluster suggests a rather strong dynamical character at finite temperature. Prediction of the lowest energy structures and electronic properties is crucially sensitive both to non-dynamical and dynamical electron correlation treatment. The CASPT2 vertical ionization energy is 3.66 eV, in excellent agreement with the 3.6 ± 0.1 eV experimental figure. All the isomers are found to have a strong multireference character, thus making Kohn-Sham density functional theory fundamentally inappropriate for these systems. Only large multiconfigurational complete active space self-consistent field (CASSCF) wavefunctions provide a reliable zeroth-order description; then the dynamic correlation effects must be properly taken into account for a truly accurate account of the structural and energetic features of alkali-metal clusters.

Introduction

Cluster science is now a well established field that has attracted the attention of many scientists since, besides addressing fundamental questions on physics and chemistry, it also provides new and promising technological developments.[1–3] A captivating aspect is that cluster science plays an important role in several, sometimes unexpected, areas: for example, in astrophysics where it was realized that clusters play an important role in the formation and properties of cosmic dust,[4] as well as the prediction and detection of carbon clusters in the interstellar medium.[5–7] This area is now important in terms of technological applications such as the design of novel nano-materials[8,9] (for electronics, photonics or magnetism) or drug delivery on specific targets in the human body.[10,11] Moreover, some transition metal clusters are known to be good catalysts as they can exhibit a large and tunable surface to volume ratio.[12,13] At the molecular scale, some interesting and unexpected phenomena have been discovered such as the pseudo-rotating Li_3, Na_3 and K_3 clusters.[14]

From all the fascinating inquiries about clusters, in particular metal clusters, the quest for the determination of the optimal molecular shape is among the most important and

difficult tasks to tackle.[15] This arises from the fact that numerous observable properties of clusters are governed by their molecular shape; nonetheless, both the nuclear framework structure and the electronic properties of a cluster are difficult to obtain by experimental means and this makes theoretical research very important for their study. Moreover, many physical and chemical properties of clusters are size-dependent, differ substantially from their bulk analog and sometimes show novel characteristics that can be modified almost at will to create nano-materials for many technological applications.[9] Identification of the geometry of a stable cluster is a must in order to calculate electronic and optical properties (e.g. polarizabilities and optical-UV or infrared spectra) and its chemical reactivity/inertness with respect to other molecules.[16,17]

Alkali-metal clusters have been the subject of many works both by experimental and theoretical means.[1,18–23] Excluding the technological applications, one of the main motivations for this research has been the fundamental question of how basic properties (internuclear distances, chemical bonding patterns, electronic excitation spectra, magnetism, and ionization energies, for instance) of homonuclear clusters evolve from the atom, the dimer and small isomers towards the bulk. Although at first sight alkali-metal clusters seem quite simple due to the fact that every atom provides just one electron to the overall valence structure of the cluster, they exhibit two interesting phenomena. First, the bonding shows a multi-center delocalized behavior rather than directional two-center bonding due to the spherical symmetry of the ns valence atomic orbitals of the alkali atoms; secondly, the potential energy surface (PES) is very flat for any given spin manifold with many shallow minima.[24] Additionally, for alkali-metal clusters of low nuclearity it has been shown that the optimal geometries of the neutral clusters ($\mathbf{R}_{eq}$) differ considerably from their anionic ($\mathbf{R}_{eq}^{-}$) or cationic ($\mathbf{R}_{eq}^{+}$) counterparts.[25] Furthermore, it has been shown that the wavefunctions can exhibit a rather large multi-reference character,[20,26–30] thus making Kohn-Sham (KS) density functional theory (DFT) inappropriate for these systems. Thus, only large multiconfigurational complete active space self-consistent field (CASSCF) wavefunctions provide a reliable zeroth-order

description.[31]

In a recent paper we have studied the three lowest spin states of the very floppy Li_{13}^+ cluster using DFT and benchmark multireference CASSCF(12,12) + CASPT2(12,12) calculations with a couple of Dunning's correlation-consistent basis sets.[31] Optimized structures and energetics were reported. We found many distinct low-energy isomers. Starting from the hybrid functional DFT optimized structures, it was found that both the topology and symmetry of the cluster were drastically changed during the geometric optimization procedure when the CASSCF approach was utilized. The Li_{13}^+ CASPT2(12,12)/cc-pVTZ lowest energy structures are a centered-squared antiprism singlet (S=0) and a quintet (S=2) icosahedron lying 3.4 kcal/mol above the former. The lowest triplet lies 5.6 kcal/mol above the singlet ground state. These results reveal two quasi-degenerate and topologically distinct isomers with different spin multiplicities. Furthermore, the rather small energy differences between various isomers suggest a strong dynamical behavior of this floppy cluster at finite temperature and actually precludes the identification of a single dominant structure for Li_{13}^+

To gain further insight both in the electronic and geometrical structures of this type of alkaline metal clusters, we focus our attention here on the energetic ordering of the different spin states of Na_{13}^+ using the multireference *ab initio* CASSCF + CASPT2 approach successfully utilized for Li_{13}^+.[31] Even though Na_{13}^+ and Li_{13}^+ have similar valence electronic structures, their properties are expected to be different due to the presence of the semi-core electrons which are absent in the lithium case.[32] We consider here the full valence space of the thirteen atoms leading to very large CASSCF(12,12) zeroth-order reference wavefunctions.

Since the early days of cluster science, when Knight *et al.* produced and detected alkali-metal clusters with up to *ca.* 100 atoms,[33] sodium clusters have received a lot of attention both experimentally and theoretically.[1,34] With these experiments Knight *et al.* proved that metal clusters have the shell electronic structure, and magic numbers were determined by observing peaks in the sodium clusters abundances in mass spectra. Many experimental electronic properties of small metal clusters, in particular sodium clusters, have been reported

over nearly four decades.[16,35] To understand the link between equilibrium conformation, electronic structure and magnetism both theory and experiment are important. Theoretically one can perform a conformational search and obtain stable structures by geometry optimization at a certain level of theory. Then, it is customary to test the optimized structures by computing an available experimental property. Thus, the predicted values of electronic properties like the binding energy per atom, dissociation energy of the cluster and ionization energy can be compared against the experimental results. Once a reliable agreement is obtained between theory and experiment, the optimized geometry of the cluster is usually regarded as the true ground state structure. For some Na_n^+ clusters comparison of experimental depletion spectra recorded at low temperature with the optical transitions theoretically determined for the stable structures allowed the identification of the cluster geometries.[16]

More that 30 years ago the cationic Na_{13}^+ cluster was observed in experiments using the liquid metal ion source (LMIS) procedure for cluster production by Saito *et al.*,[36] and determined to be (among others) a magic number cluster. Nevertheless, the special stability of the Na_{13}^+ cluster cannot be explained by the spherical or through the ellipsoidal jellium model. This unsatisfying situation shows the importance of atomic structure which is neglected in the jellium model in the prediction of cluster stability and other physicochemical properties. From the theoretical point of view, since the mid 80s an extensive search of low-energy isomers has taken place on the PES of cationic Na_{13}^+. The majority of studies used DFT with different approximations to the exchange-correlation (XC) functional and, in some studies, using pseudopotentials. More recently, single-reference diffusion Monte Carlo (DMC) results have also been reported.[37–42]

We emphasize here that, in spite of the plethora of studies, no agreement regarding the lowest energy structure of this cluster has been reached. For instance, in order to obtain equilibrium geometries without imposing any symmetry constraints, Martins and Buttet[37] used LDA-DFT and started from randomly generated geometries; they concluded that a slightly distorted cubo-octahedron (doublet spin state for the neutral cluster or singlet spin

state for the cationic cluster) rather than the icosahedron (hexuplet spin state for the neutral cluster or quintet for the cationic cluster) are the lowest energy configurations at this level of theory for the Na_{13} and Na_{13}^+ clusters. Iñiguez et al.[38] used pseudopotential LDA-DFT starting from about fifteen initial geometries to determine the ground state and low-lying structures of X_n (X=Na, Mg, Al and Pb) clusters with $n <\sim 50$. In the particular case of Na clusters, they also performed selected computations on the singly charged Na_n^+ (n=8-14) clusters. One of their conclusions is that these calculations predict that 13-atom clusters have an icosahedral structure and a high stability with respect to neighbor sizes. Moreover, Lopez et al.[39] using the same LDA approach as in [38] but starting from educated guesses of ca. 50 geometries found, once again, that the lowest energy isomer both of Na_{13} and Na_{13}^+ is the icosahedron. Calvo et al.[40] performed a systematic and unconstrained global optimization by the basin-hopping method with three different energy functions: a modified many-body empirical classical potential, a simple quantal Hückel-type model, and a LDA-DFT based orbital-free model in order to determine the lowest-energy minimum of cationic sodium clusters Na_n^+ with $n \leq 40$. In the particular case of Na_{13}^+ they found that the structure of the lowest energy isomer is strongly method-dependent: both an ICO structure with I_h symmetry or a cluster based on capping isolated atoms over a fivefold symmetric seed (their fig. 1b) with C_{3v} symmetry were obtained as the lowest energy isomers. Furthermore, Solov'yov et al.[41] carried out a systematic and intensive study using the single-reference B3LYP-DFT approach of neutral and cationic sodium clusters for N$\geq$ 7. They ended up with the same optimal structure both for the neutral Na_{13} and for the cationic Na_{13}^+ clusters: a low symmetry (C_1) structure (their fig. 2) with doublet spin state for the neutral cluster and singlet spin state for the cationic cluster.

One of the most recent studies was reported by Hsing et al.[42] through systematic GGA-DFT and single-reference DMC calculations of the relative energies of 13-atom metal clusters, including sodium. For neutral clusters they studied nine different representative isomers; in addition they performed DFT and DMC computations for cationic clusters, they removed

a single electron from the highest occupied molecular orbital (HOMO) of the two lowest-energy optimized neutral clusters of each element and carried out geometry optimizations with GGA-DFT. They concluded that the lowest energy isomer both of Na_{13} (2S+1=2) and Na_{13}^+ (2S+1=1) is their T13 (or GCL-Garrison cap layer) structure.

It is now well known that different XC functionals can yield wrong and unreliable structural predictions since the wavefunctions of this alkali-metal clusters have a rather large multi-configurational character. Thus, it is not surprising that very different optimal structures are obtained using various types of DFT approximations. Overall, the rather flat topology of the potential energy surfaces for the various spin manifolds, the delocalized character of the non-directional bonding, the exceedingly large number of possible isomers, the multiconfigurational nature of the wavefunctions and the absence of a clear guide to determine the ground-state geometry makes the elucidation of the ground-state structure of Na_{13}^+ a highly difficult task.

In this article we present hybrid DFT and benchmark multireference studies of the three lowest spin states of the Na_{13}^+ cluster in order to determine their optimal structures, their energetic hierarchy, and the magnetic vs. non-magnetic nature of the ground state. As an excellent starting point, we use our recently reported geometries of Li_{13}^+.[31] Furthermore, we examine other structures previously reported in the literature, namely, the C_1 symmetry isomer of Solov'yov et $al.$[41] (here denoted as C1-Solov), the GCL of Hsing et $al.$,[42] a perfect cuboctahedron with O_h symmetry and a previously reported optimal isomer for the neutral Na_{13} cluster by Poteau and Spiegelmann with C_1 symmetry (here denoted as C1-Poteau).[43] The latter particularly stable isomer consists of a pentagonal bi-pyramidal (PBP) seed with three capping atoms lying above the PBP basis plane and three below (i.e. a 3:3 capping pattern). We evaluate quantitatively the reliability of the hybrid DFT approach by comparing the results with those of highly correlated wavefunction methods. Fully unrestricted geometry optimizations are done at the CASSCF(12,12)/cc-pVDZ level of theory. We report the structure of low energy isomers, their relative energies, and ionization energies.

Computational details

All the DFT and CASSCF(12,12) computations were carried out using the *Gaussian-09* package.[44] The Kohn-Sham DFT calculations used the hybrid PBE0,[45] B3LYP[46–48] and M06-2X[49] exchange-correlation functionals as programmed in G09. These calculations were performed with the 6-31G*[50] basis set and with the correlation consistent cc-pVDZ and cc-pVTZ basis sets of Dunning et al.[51] On the other hand the benchmark CASSCF optimizations utilized only the cc-pVDZ and cc-pVTZ basis sets. Due to the f-type ($l = 3$) orbitals included in the cc-pVTZ basis set, achieving full CASSCF convergence was often tricky and sometimes impossible, thus we decided to exclude the f-orbitals and utilize instead the resulting (16s10p2d) basis set contracted to [5s4p2d], which leads here to a basis of 351 molecular orbitals for Na_{13}^+. We will denote the cc-pVTZ basis set without the f-orbitals as cc-pVTZ*. No symmetry constraints were imposed during the geometric optimizations. The CASSCF(12,12)/cc-pVDZ optimizations were carried out starting from the optimized PBE0 geometries and from the previously mentioned structures obtained by us and other authors for all spin states. The dynamical correlation effects were introduced through CASPT2(12,12)/cc-pVDZ and CASPT2(12,12)/cc-pVTZ* computations with the Molpro-2012[52] code. A level shift of 0.20 Hartree was applied to the zeroth order Hamiltonian in all CASPT2 calculations to avoid intruder states that might originate from quasidegeneracies in the zeroth-order Hamiltonian spectrum.

The large CASSCF(12,12) wavefunctions were used as references for the CASPT2 computations leading to huge spaces with up to 3.3×10^{10} uncontracted Configuration State Functions (CSF) for the CASPT2(12,12)/cc-pVTZ* calculations. Table 1 presents the number of contracted/uncontracted CSF in the CASSCF and CASPT2 computations with the cc-pVDZ and cc-pVTZ* basis sets for the three lowest spin states of the cationic cluster as well as for the doublet spin state of the neutral cluster.

The default values of the geometric convergence criteria were used in both DFT and CASSCF computations. A self-consistent field convergence of 10^{-6} a.u. was used in all

Table 1: Number of contracted/uncontracted Configuration State Functions (cCSF,uCSF) in the CASSCF and CASPT2 computations with the cc-pVDZ and cc-pVTZ* basis sets

Na_{13}^+	S=0	S=1	S=2
CASSCF(12,12)			
CSF	226 512	382 239	196 625
CASPT2(12,12)			
cCSF(cc-pVDZ)	55 345 758	99 954 465	61 242 935
uCSF(cc-pVDZ)	5 627 973 780	10 891 362 339	7 384 106 015
cCSF(cc-pVTZ*)	98 730 060	176 466 147	109 044 221
uCSF(cc-pVTZ*)	17 083 421 784	33 076 768 725	22 445 017 595

Na_{13}	S=1/2
CASSCF(13,13)	
CSF	1 288 287
cCSF(cc-pVDZ)	319 160 049
uCSF(cc-pVDZ)	34 587 745 335

CASSCF calculations while the default 10^{-8} a.u. threshold was used in all DFT calculations. For the DFT calculations the UltraFine grid as implemented in Gaussian-09 was utilized. The default SCF convergence criteria of Molpro-2012 were used in all the single-point CASPT2(12,12)/cc-pVDZ computations, this corresponds to a 10^{-6} a.u. convergence threshold for the energy, while a 10^{-4} a.u. threshold was set for all the CASPT2(12,12)/cc-pVTZ* calculations.

Due to the expected closeness in energy between isomers it is important to include the zero-point energy (ZPE) correction to the Born-Oppenheimer (BO) energies. Frequency calculations with the CASSCF(12,12) method cannot be performed due to the computational cost of the analytic second derivatives with such large multireference wavefunctions. Since the CASSCF vibrational frequencies are unattainable we have decided to use, as a first approximation, the computed ZPE corrections at the PBE0/cc-pVTZ level of theory. However, such DFT vibrational frequencies must be taken with caution due to the large multireference character of the wavefunctions of this system.

More than 43 years ago Herrmann, Schumacher and Wöste measured the ionization energy (IE) of various Na_N clusters, with $N \leq 14$.[53] They stress that even though their measurements may be interpreted as adiabatic ionization energies, vertical and adiabatic ionization energies are indistinguishable with the resolution of their method. More recently, de Heer *et al.* have reported experimental IE's of sodium clusters from photoionization efficiency spectra.[1] In the particular case of Na_{13} the experimental IE of both studies are identical, 3.6 ± 0.1 eV which we shall compare against our computed IE of the neutral cluster.

Let us recall that, neglecting ZPE corrections, the so-called adiabatic IE (AIE), is the energy required to take the cluster from the most stable neutral isomer to the most stable cationic isomer. That is, the energy difference between the global minimum of the ground state adiabatic PES' $E_0^+(\mathbf{R}_{eq}^+)$ and $E_0(\mathbf{R}_{eq})$ of the cationic and neutral systems, respectively:

$$\text{AIE} = E_0^+(\mathbf{R}_{eq}^+) - E_0(\mathbf{R}_{eq}). \tag{1}$$

The vertical IE (VIE) is the energy difference without nuclear relaxation after ionization,

$$\text{VIE} = E_0^+(\mathbf{R}_{eq}) - E_0(\mathbf{R}_{eq}). \tag{2}$$

In order to obtain an estimate for the IE we need to know the ground state structure of Na_{13}. The neutral Na_{13} cluster has been the subject of many studies.[38,39,41,43,54–57] A careful analysis of these reports reveals that the 3:3 capped PBP structure of Poteau and Spiegelmann with doublet spin state seems to be the ground state configuration of this neutral cluster. Nevertheless, to best of our knowledge, no multireference *ab initio* study has ever been reported. Due to the single-configurational wavefunction ansatz of all the previous investigations, multireference *ab initio* computations are needed to shed light on the true energy hierarchy of the different isomers of Na_{13} at $T = 0$ K.

Results

Hybrid DFT

Twelve different configurations were found as stationary points on the PES of the three lowest spin states we explored. Sometimes both the symmetry and topology of the cluster dramatically changed during the geometry optimization procedure for each spin state for the three XC-functionals and three basis-sets utilized here. As expected, optimized geometries are dependent on both the XC functional and the basis set utilized. For instance, the singlet CSAP-(1,3) optimized geometry with the B3LYP functional is basis set-dependent. However, for this CSAP-(1,3) singlet, the optimized PBE0 and M06-2X geometries are nearly identical and independent of the basis set utilized. For the CSAP-(1,3) triplet the optimized geometry at the M06-2X/cc-pVTZ level that starts from the CSAP-(2,2) isomer gets quite distorted and becomes a cage-like structure, very similar to the buckled biplanar (BBP) isomer that Chang and Chou found for late transition metals with more than half-filled d shells.[58] On the other hand the same optimized geometry but at the PBE0/cc-pVTZ level becomes a capped PBP (here labeled as PBPc). All the optimized structures for the three spin states are presented in the Supplementary Material and only the PBE0/cc-pVTZ optimized geometries are shown in figure 1. We note that the optimized geometries obtained at the PBE0/cc-pVTZ level are, with the minor exception of the triplet CSAP-(1,3) discussed above, qualitatively identical to those predicted with the M06-2X/cc-pVTZ approach.

CSAP-(1,3);S=0   CSAP-(1,3);S=1   CSAP-(2,2);S=0   PBPc;S=1

ICO; S=1   ICO; S=2   A.1; S=1   OPTET(I); S=0

OPTET(II); S=0   C1-Solov; S=0
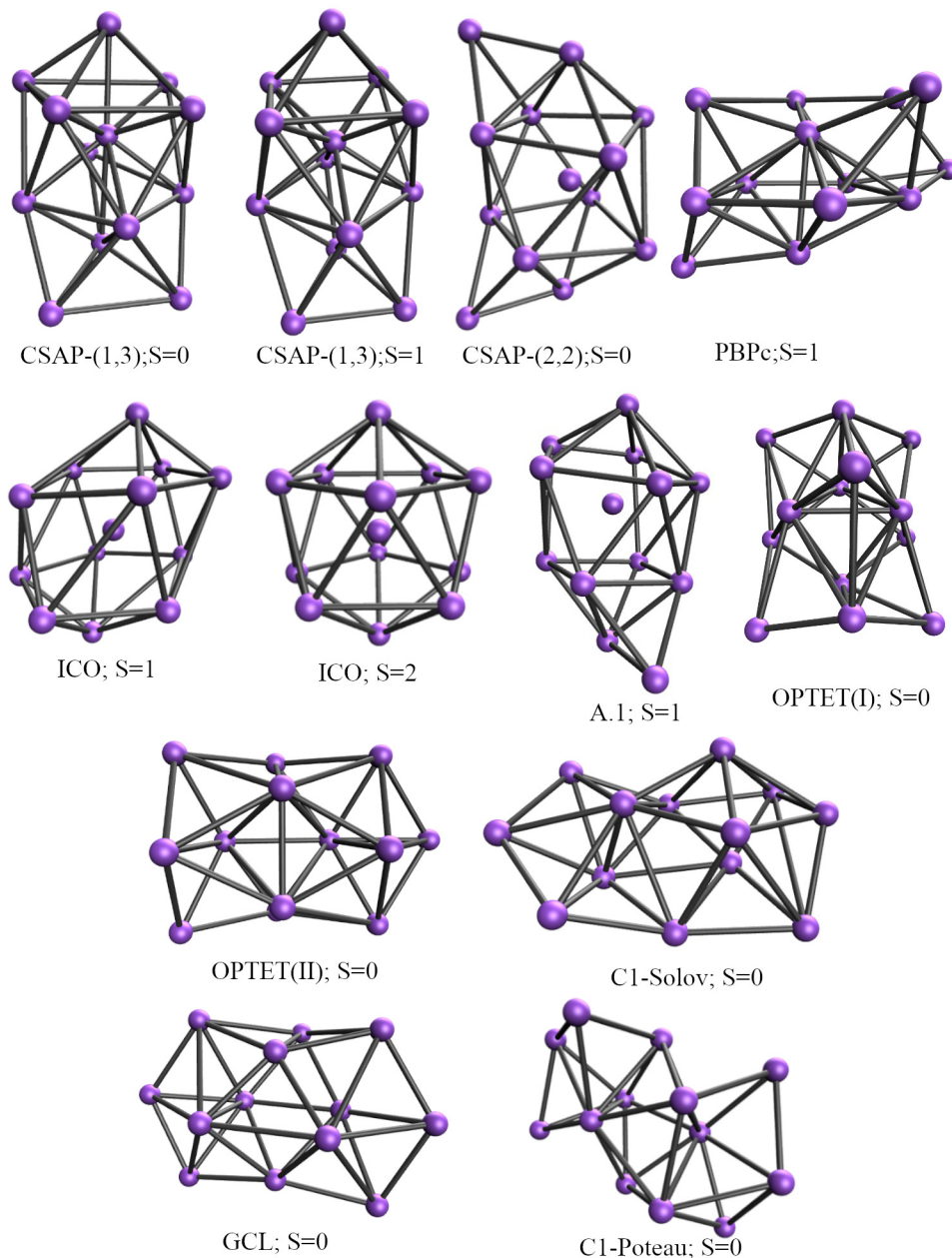
GCL; S=0   C1-Poteau; S=0

Figure 1: PBE0/cc-pVTZ optimized geometries.

Relative energies using the PBE0 and M06-2X functionals are reported in tables 2 and 3 with the 6-31G* and cc-pVTZ basis sets, respectively. At this level of theory the lowest energy isomer is XC functional and basis set independent: the singlet OPTET(II) is obtained both with the PBE0 and M06-2X XC functionals. Although there are some quantitative differences between the results depending on the XC-funcional and basis set utilized,

Table 2: Relative energies (kcal/mol) with hybrid exchange-correlation DFT methods using the 6-31G* basis set. The Hessian index (HI) is shown for each optimized structure.

Isomer	2S+1	PBE0 ΔE	PBE0 HI[a]	M06-2X ΔE	M06-2X HI[a]
OPTET(II)	1	0.0	0	0.0	0
C1-Poteau	1	1.0	0	0.9	0
CSAP-(1,3)	1	1.3	0	2.2	0
C1-Solov	1	1.8	0	1.7	0
CSAP-(2,2)	1	2.2	0	3.6	0
GCL	1	2.2	0	2.1	0
CSAP-(1,3)	3	2.6	0	3.2	0
A.1	3	3.4	0	3.6	0
ICO	5	5.6	0	3.2	0
OPTET(I)	1	6.9	0	8.2	0
ICO	3	7.7	0	-[b]	-
CSAP-(2,2)	3	7.9	0	9.5	0

[a] Number of imaginary frequencies.
[b] Unstable structure.

Table 3: Relative energies (kcal/mol) with hybrid exchange-correlation DFT methods using the cc-pVTZ basis set. The Hessian index (HI) is shown for each optimized structure..

Isomer	2S+1	PBE0 ΔE	PBE0 HI[a]	M06-2X ΔE	M06-2X HI[a]
OPTET(II)	1	0.0	0	0.0	0
C1-Poteau	1	1.1	0	1.0	0
CSAP-(1,3)	1	1.9	1	1.6	0
C1-Solov	1	1.6	0	1.6	0
CSAP-(2,2)	1	2.7	0	3.7	0
GCL	1	2.0	0	2.0	0
CSAP-(1,3)	3	3.2	-[b]	4.3	0
A.1	3	3.8	0	4.6	0
ICO	5	7.3	0	7.0	2
OPTET(I)	1	7.0	0	8.0	0
ICO	3	8.2	2	9.9	4
PBPc	3	7.2	0	-	-
BBP	3	-	-	7.8	0

[a] Number of imaginary frequencies.
[b] Frequency job did not converge.

the overall picture is roughly the same at each level of theory, i.e., a very flat PES with many shallow minima. Here we stress that the character of the stationary points is XC functional-dependent; however, this should not come as a surprise given the large multireference character of the Na_{13}^+ cluster. Furthermore, the inclusion of the ZPE correction to the Born-Oppenheimer energies does not substantially alter the relative energies.

In the following, unless otherwise stated, we shall discuss only the results obtained at the PBE0/cc-pVTZ level of theory. The lowest energy structure is the singlet OPTET(II) but there are at least 7 low-lying isomers within an energy range of only 3.8 kcal/mol. This large variety of nearly degenerate isomers confirms the extremely flat topology of the PES. The lowest triplet [CSAP-(1,3)] and the lowest quintet (ICO) lie higher in energy than our lowest minimum by 3.2 and 7.3 kcal/mol, respectively. It is important to emphasize that, in contradiction with previous lower level of theory (LDA and GGA-based) studies, the highly symmetrical icosahedron is among the highest lying energy isomers for all the spin states; the triplet and quintet structures become rather deformed ICO, although the quintet state has C_i symmetry. This instability of the low-spin states of the ICO structure is clearly due to the Jahn-Teller effect. The ICO triplet and quintet spin states lie higher in energy than our lowest singlet by 8.2 and 7.3 kcal/mol, respectively. We stress that our goal using Kohn-Sham DFT for this multireference system is, by no means, to obtain accurate relative energies between isomers and spin states, but to gauge the performance of the different XC-functionals and basis sets to compare these with the highly correlated CASSCF and CASPT2 results in the following section.

In order to estimate the ionization energies, we have performed three PBE0/cc-pVTZ geometry optimizations for the neutral cluster: ICO[S=5/2], C1-Poteau[S=1/2] and GCL[S=1/2].[42] The lowest energy isomer turned out to be the C1-Poteau doublet spin state configuration, the doublet GCL and hextuplet ICO lie 1.60 and 2.92 kcal/mol above the C1-Poteau isomer, respectively. Then, we assume the C1-Poteau doublet (S=1/2) as the global minimum of Na_{13}. With the electronic energies of the latter computation and of our lowest energy struc-

ture for the singly charged cluster we computed the AIE. On the other hand, in order to obtain the electronic energy needed to compute the VIE we removed one electron from the HOMO of the neutral ground state structure, then we performed a single point PBE0/cc-pVTZ computation. VIE and AIE at the PBE0/cc-pVTZ level of theory are reported in table 4

Table 4: Ionization energies (eV) considering the C1-Poteau lowest energy doublet (S=1/2) as the ground state of Na_{13}.

PBE0/cc-pVTZ		
Adiabatic[a]	Vertical	Experimental[b]
3.62	3.75	3.6 ± 0.1

[a] OPTET(II) used as the ground state of Na_{13}^+.
[b] Experimental structure is not known[1,53]

Our PBE0/cc-pVTZ IEs agree rather well with the experiment. However, as we shall see below, this actually arises due to a serendipitous cancellation of errors given the strong multireference character of the wavefunctions for all spin states, which lead to rather different optimal structures when the non-dynamical correlation effects are properly taken into account through the CASSCF(12,12) approach.

Multireference *ab initio* CASSCF-CASPT2 results

Full CASSCF(12,12)/cc-pVDZ geometry optimizations were done starting from the PBE0/6-31G* level optimized geometries. We also performed one geometry optimization starting from the CSAP-(1,3) singlet obtained at the M06-2X/cc-pVTZ level of theory. After the CASSCF geometry optimization the latter isomer relaxed into a structure formed by two PBPs fused together sharing one atom (henceforth denoted as PBPb). However, the CASSCF optimized geometry starting from the PBE0/6-31G* isomer remained a CSAP-(1,3) structure, even though the CSAP(1,3) optimized geometries at the PBE0/6-31G* and M06-2X/cc-pVTZ levels are nearly identical. This reveals a strong dependence of the CASSCF optimized geometries on the initial configuration. Optimized geometries at the

CASSCF(12,12)/cc-pVDZ level of theory are shown in figure 2. The triplet (S=1) CSAP-(2,2) is not stable at CASSCF(12,12)/cc-pVDZ level and relaxed into two PBPs fused together capped with four atoms (henceforth denoted as PBPa). Furthermore, both the C1-Solov and the GCL structures get quite distorted. The geometrical distortion of the triplet ICO is considerably less pronounced than with PBE0/cc-pVTZ. For the PBPa singlet isomer the CASSCF(12,12)/cc-pVDZ geometry optimization required 684 CPU days on 64 processors, while the geometry optimization at the same level of theory for the ICO quintet took 85 CPU days. Once the optimal geometries were determined at the CASSCF(12,12)/cc-pVDZ level, we proceeded to perform single-point CASPT2(12,12) calculations both with the cc-pVDZ and the much larger cc-pVTZ* basis set. The CASPT2(12,12)/cc-pVTZ* computations required from 20 to 60 CPU days depending on the type of structure and the spin state.
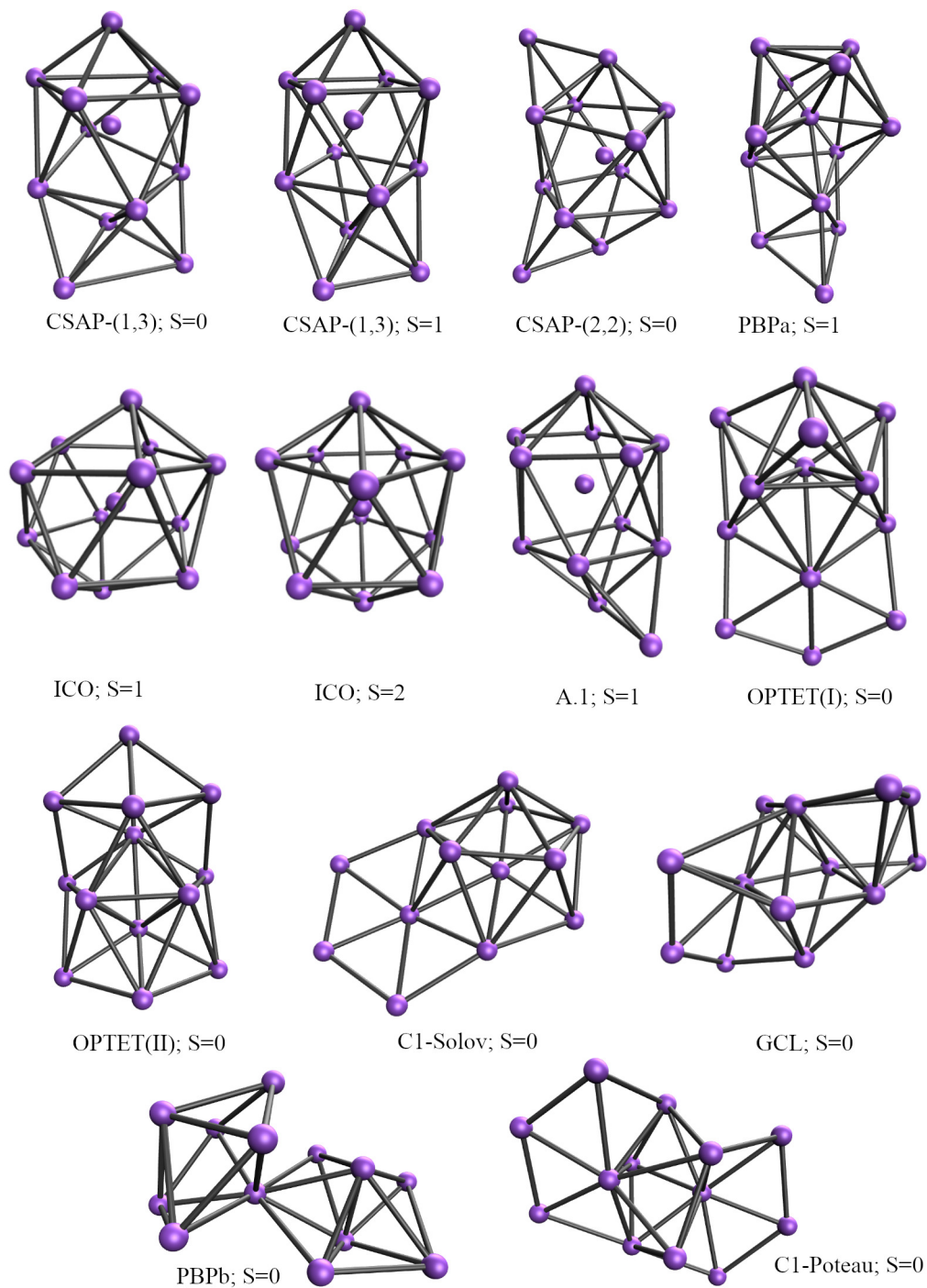
Figure 2: CASSCF(12,12)/cc-pVDZ optimized geometries.

Table 5 presents the composition of the optimized CASSCF(12,12)/cc-pVTZ* wavefunctions of the three lowest spin states at the CASPT2(12,12)/cc-pVTZ* level, where many CSF appear with CI coefficients larger than 0.05 in absolute value. Note the very low

0.85*0.85=0.72, 0.85*0.85=0.72 and 0.86*0.86=0.74 weights of the reference configurations for the singlet, triplet and quintet states, respectively. Moreover, CASSCF(12,12)/cc-pVTZ* natural occupation numbers of the lowest singlet, triplet and quintet states are shown in table 6. The multireference character of the wavefunctions is also shown in these natural occupation numbers, where non-negligible fractions of electrons are present in the originally-virtual orbitals when they are included in the active space for all the spin states. We also show the occupation numbers with their energy levels diagrams for the lowest three spin states in the figure 3.

Table 5: List of leading configurations in second-quantized form with the CI coefficients larger than 0.05 in the CASSCF(12,12)/cc-pVTZ* wavefunctions of the three lowest energy spin states obtained at the CASPT2(12,12)/cc-pVTZ* level.

S=0 [PBPb]		S=1 [CSAP-(1,3)]		S=2 [ICO]	
CSF	CI coefficient	CSF	CI coefficient	CSF	CI coefficient
222222000000	0.8544800	22222aa00000	0.8505773	2222aaaa0000	0.8594649
220222000200	-0.1007956	22220aa20000	-0.1267818	222aaaab00a0	0.1375915
222220200000	-0.0951685	2222abaa0000	-0.1086581	222aa0a2000a	0.1064200
222022200000	-0.0920787	222a2ab00a00	-0.0875817	22a22a0aa000	-0.0972610
222202020000	-0.0797967	2a222baa0000	-0.0870999	222aa2a0000a	-0.0946237
222202002000	-0.0788427	22022aa02000	-0.0730160	22a20a2aa000	0.0932073
222202000020	-0.0776237	22022aa00020	-0.0718831	222aa20aa000	0.0910801
222220000002	-0.0636228	22202aa00002	-0.0675421	2a2220aaa000	0.0895426
222220ba0000	-0.0609294	22a22ba0a000	-0.0668191	2202aaaa0200	-0.0878847
222220ab0000	0.0609294	22022aa00002	-0.0633060	2a2202aaa000	-0.0869564
222220020000	-0.0604104	22202aa00200	-0.0584647	222aa02aa000	-0.0840554
222022002000	-0.0598316	22202aa00020	-0.0567897	2a222a0a00a0	0.0785845
22b2a2000200	0.0564311	2a222aab0000	0.0565301	222aaaba00a0	-0.0627029
22a2b2000200	-0.0564311	2b222aaa0000	0.0559142	2022aaaa0200	-0.0610750
222022000002	-0.0528537	2a222ba00a00	0.0524637	2a22abaa000a	0.0579232
222220000020	-0.0528098	2222baaa0000	0.0518874	2aa22aaa0b00	0.0573708
2222bab0a000	-0.0526332	22aa2aa000bb	0.0504493	2a22a2a000a0	-0.0573404
2222aba0b000	-0.0526332	2222aaab0000	0.0501527	2220aaaa0020	-0.0549743
				22a2a02a000a	-0.0530653
				2222a0a000aa	-0.0525992
				2a22aaa00b0a	0.0517366
				22a220aa00a0	-0.0501926

The present results highlight the unreliability of all the previous DFT Kohn-Sham de-

Table 6: Natural occupation numbers of the active orbital space at the CASSCF(12,12)/cc-pVTZ* level of theory. Where it is conspicuous clear that fractions of electrons are present in the originally-virtual orbitals when they are included in the CASSCF(12,12) active space.

Orbital	S=0 [PBPb] Nat. Occ.	S=1 [CSAP-(1,3)] Nat. Occ.	S=2 [ICO] Nat. Occ.
1	1.98346	1.97119	1.96970
2	1.94320	1.89705	1.89533
3	1.90262	1.88100	1.89191
4	1.87008	1.87494	1.87837
5	1.84503	1.84480	1.00981
6	1.82149	1.00549	0.99827
7	0.16519	0.99573	0.99803
8	0.13199	0.14836	0.99280
9	0.10757	0.10631	0.10018
10	0.09510	0.10032	0.09887
11	0.08504	0.09312	0.08857
12	0.04925	0.08168	0.07814

scriptions for this type of clusters due to the rather strong multireference character of the wavefunctions for all the spin states explored here. The weights of the leading CI configurations in the CASSF(12,12)/cc-pVTZ* description are listed in table 7 and 8. Without question, even the largest weights are significantly smaller than what would be expected for a single-reference system. Thus, Na_{13}^+ cannot be properly described by any quantum chemical treatment based on a single-reference method.
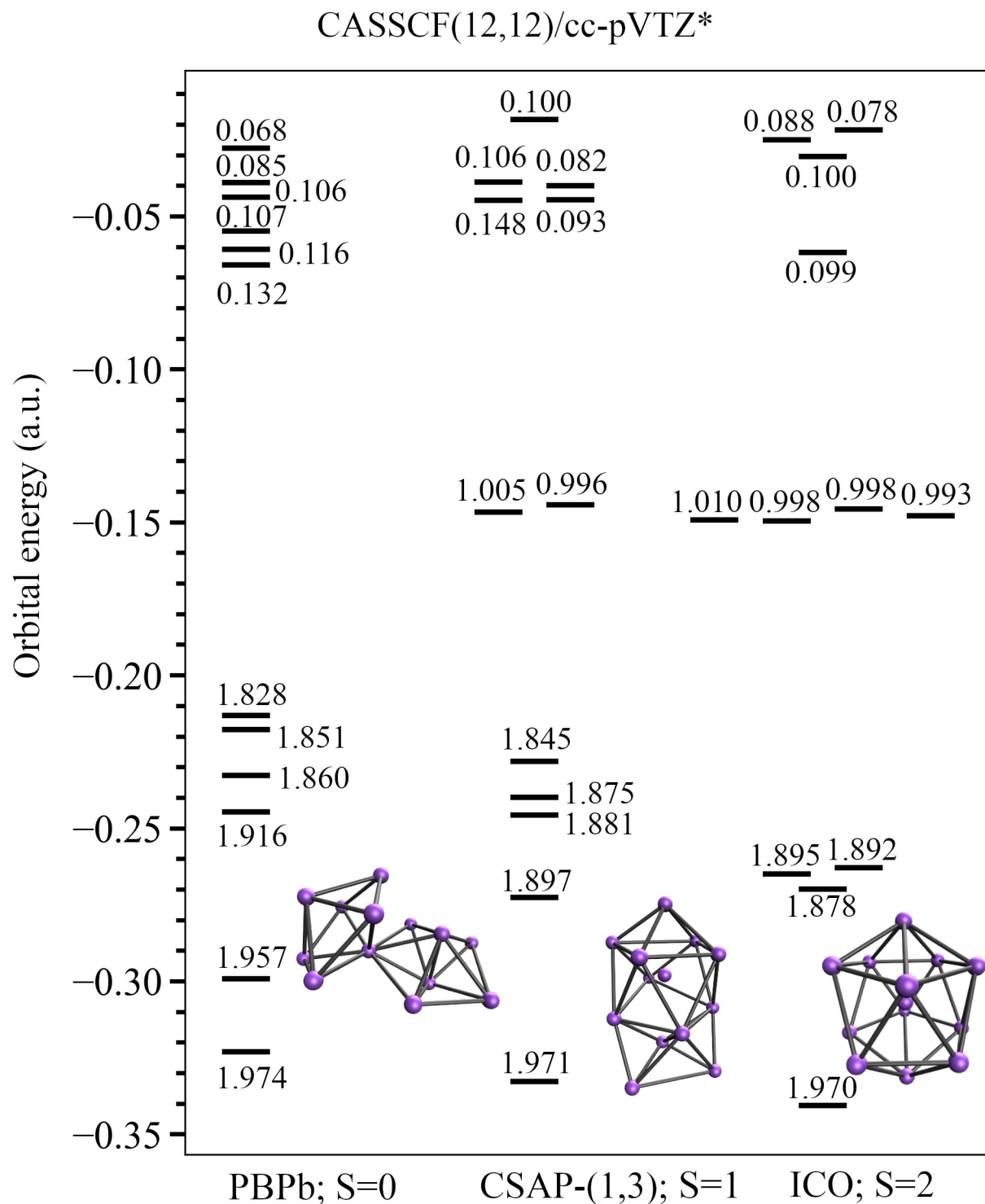
Figure 3: Orbital energies of the active space with the natural occupation numbers at the CASSCF(12,12)/cc-pVTZ* level. As insets we show the CASSCF(12,12)/cc-pVDZ optimized geometry of the corresponding spin state.

In table 7 we present the CASSCF(12,12)/cc-pVDZ and CASPT2(12,12)/cc-pVDZ relative energies. The CASSCF(12,12)/cc-pVTZ* and CASPT2(12,12)/cc-pVTZ* relative energies are presented in table 8.

Table 7: CASSCF(12,12)/cc-pVDZ and CASPT2(12,12)/cc-pVDZ relative energies for Na_{13}^+ optimized isomers.

| Isomer | 2S+1 | CASSCF(12,12) | | CASPT2(12,12) |
		ΔE^a	c_0^2 [b]	ΔE^a
C1-Poteau	1	0.00	0.61	8.80
OPTET(I)	1	0.39	0.65	8.61
GCL	1	1.18	0.72	8.82
PBPb	1	2.87	0.73	0.00
C1-Solov	1	3.18	0.72	6.07
CSAP-(1,3)	1	3.78	0.75	1.04
OPTET(II)	1	4.43	0.72	1.53
CSAP-(2,2)	1	5.10	0.74	4.00
PBPa	3	7.61	0.79	10.12
CSAP-(1,3)	3	7.83	0.72	4.50
A.1	3	9.66	0.75	5.06
ICO	5	13.12	0.74	3.30
ICO	3	18.25	0.53	10.88

[a] In kcal/mol^{-1}.
[b] c_0^2 is the CI coefficient squared of the reference determinant.

The inclusion of the dynamical electron correlation turned out to be crucial. The relative energies are significantly modified when considering the second order perturbation correction on top of the non-dynamical electron correlation taken into account with CASSCF(12,12). The lowest energy isomer is method dependent: it is the C1-Poteau structure with the CASSCF(12,12) method but it becomes CSAP-(1,3) with the CASPT2(12,12) method. The former lies *ca.* 9 kcal/mol higher in energy when taking into account the PT2 correction both with cc-pVDZ and cc-pVTZ* basis sets. Similarly, the OPTET(II) undergoes an energy lowering of *ca.* 3.8 kcal/mol with the CASPT2 correction both with cc-pVDZ and cc-pVTZ* basis sets. On the other hand, the ICO structure of the highest spin state (S=2) becomes significantly more stable (*ca.* 10 kcal/mol) with the CASPT2 method than the predicted values with the CASSCF(12,12) approach with both basis sets. The CASPT2(12,12)/cc-pVDZ and

Table 8: CASSCF(12,12)/cc-pVTZ* and CASPT2(12,12)/cc-pVTZ* single-point relative energies for Na_{13}^+ CASSCF(12,12)/cc-pVDZ optimized isomers.

| Isomer | 2S+1 | CASSCF(12,12) | | CASPT2(12,12) |
		ΔE^a	c_0^2 [b]	ΔE^a
C1-Poteau	1	0.00	0.61	8.79
OPTET(I)	1	0.31	0.65	8.60
GCL	1	1.00	0.71	8.60
PBPb	1	3.01	0.73	0.00
C1-Solov	1	3.26	0.72	5.96
CSAP-(1,3)	1	3.83	0.75	0.88
OPTET(II)	1	4.58	0.72	1.63
CSAP-(2,2)	1	5.21	0.74	3.77
PBPa	3	7.72	0.79	9.85
CSAP-(1,3)	3	8.03	0.72	4.33
A.1	3	9.85	0.75	4.96
ICO	5	13.55	0.74	3.77
ICO	3	18.57	0.52	11.30

[a] In kcal/mol^{-1}.
[b] c_0^2 is the CI coefficient squared of the reference determinant.

CASSCF(12,12)/cc-pVDZ + CASPT2(12,12)/cc-pVTZ* relative energies are nearly (within 0.44 kcal/mol) identical. There are many low energy isomers considering the relative energies obtained at the CASPT2(12,12)/cc-pVTZ* level: the absolute minimum is the singlet (S=0) PBPb, nevertheless the CSAP-(1,3) and OPTET(II) singlets lie only 0.88 and 1.33 kcal/mol above the absolute minimum, respectively. This reveals three quasi-degenerate topologically distinct isomers. The lowest triplet is a CSAP-(1,3) structure and the lowest quintet is an ICO, lying 4.33 and 3.77 kcal/mol above the singlet global minimum, respectively. Furthermore, there are two close-lying but topologically different triplet isomers, namely the CSAP-(1,3) and A.1 structures. As far as we know the PBPb isomer has not been previouly reported for Na_{13}^+. Overall the present multireference benchmark results reveal the extremely flat PES of the Na_{13}^+ cluster, a fact which precludes the identification of a single dominant structure at finite temperature.

In figure 5 we present the natural orbitals of the CASSCF(12,12)/cc-pVDZ active space of the singlet CSAP-(1,3) isomer. For the sake of comparison we also present the natural

orbitals at the PBE0/cc-pVTZ level of theory in figure 4. It can be readily seen that both the energy levels patterns and natural orbitals differ considerably from the PBE0/cc-pVTZ to the CASSCF(12,12)/cc-pVDZ level of theory. Furthermore, as already stated for other isomers in table 6 the CASSCF natural occupations numbers differ considerably from 0 or 2. In this closed shell case there are five originally-virtual orbitals with *ca.* 0.10 electrons each when they are included in the active space.
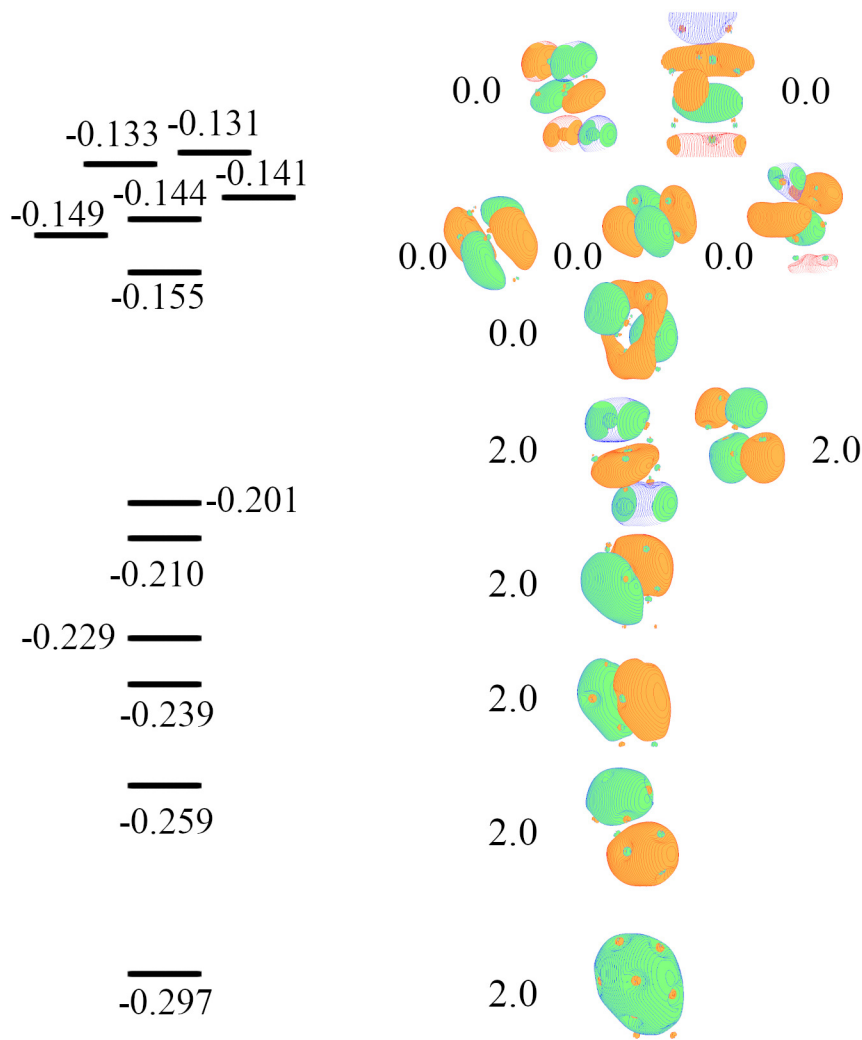

Figure 4: PBE0/cc-pVTZ natural orbitals of the singlet CSAP-(1,3) isomer: energy levels with their energy in Hartree and the plots of the natural orbitals with their natural occupation number. An isosurface value of 0.014 was utilized.
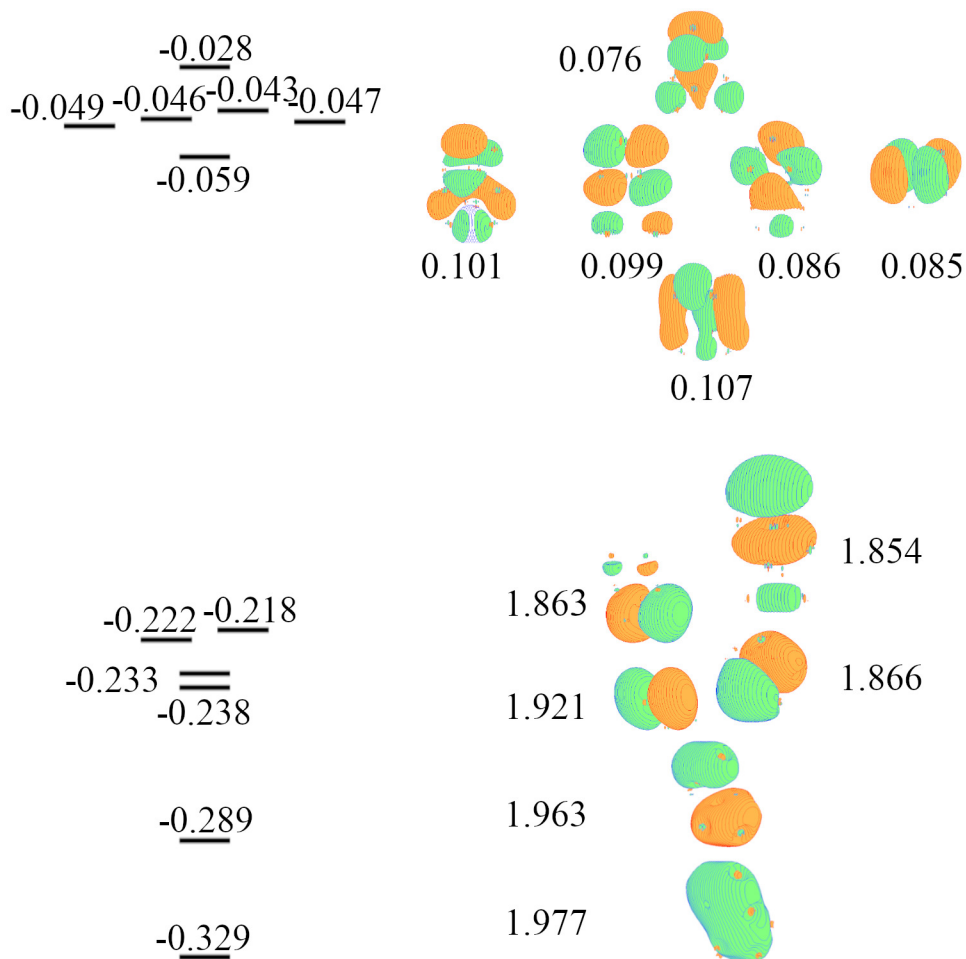
Figure 5: CASSCF(12,12)/cc-pVDZ natural orbitals of the singlet CSAP-(1,3) isomer: energy levels with their energy in Hartree and the plots of the natural orbitals with their natural occupation number. An isosurface value of 0.014 was utilized.

In order to compute the IEs with our multireference approach we first carried out a CASSCF(13,13)/cc-pVDZ geometry optimization starting from the Na_{13} doublet C1-Poteau PBE0 optimized geometry, the global minimum for the Na_{13} PES. This CASSCF optimization took 1010 CPU days. Then we computed the CASPT2(13,13)/cc-pVDZ electronic energy, next an electron was removed from the HOMO of the latter structure to obtain the CASPT2(12,12)/cc-pVDZ (S=0) electronic energy for the cationic cluster. With the latter two energies the VIE is computed. Finally, the AIE is calculated with the CASPT2(12,12)/cc-pVDZ and CASPT2(13,13)/cc-pVDZ electronic energies of the cationic and neutral global minima, respectively. The AIE and VIE are reported in table 9. Ioniza-

tion energies with the cc-pVTZ* basis set are not computed because the number of CSFs with this basis set leads to intractable CASPT2(13,13) computations needed to obtain the energy of the neutral cluster.

Table 9: Ionization energies (eV) considering C1-Poteau doublet (S=1/2) as the ground state of Na_{13}.

CASPT2/cc-pVDZ		
Adiabatic [a]	Vertical	Experimental[1,53]
2.42	3.66	3.6 ± 0.1

[a] Using PBPb as the ground state of Na_{13}^+.

The CASPT2 VIE is in excellent agreement with the experimental figure; there is a large difference (1.24 eV), between AIE and VIE due to the rather different geometrical equilibrium structures of the cationic and neutral clusters.

To summarize, in table 10 we show the hybrid DFT (PBE0) *vs. ab initio* comparison of the relative energies of the lowest energy isomers obtained in this study.

Table 10: DFT *vs. ab initio* lowest energy isomers

Isomer	2S+1	PBE0/cc-pVTZ ΔE	CASPT2(12,12)/cc-pVTZ* ΔE
PBPb	1	-	0.00
OPTET(II)	1	0.0	1.63
CSAP-(1,3)	3	3.2	4.33
ICO	5	7.3	3.77

Even though the optimized geometries obtained at the PBE0/cc-pVTZ and CASPT2(12,12)/cc-pVTZ* levels are qualitatively very similar, the energetic orderings are not. With the *ab initio* approach the ICO quintet is lower in energy than the CSAP-(1,3) triplet, while the exact opposite is predicted with the PBE0/cc-pVTZ method. Here we stress that our conformational search for low energy isomers was by no means exhaustive; i.e. we considered our previous optimal geometries of Li_{13}^+ as well some geometries of Na_{13} and Na_{13}^+ previously reported by others. Nevertheless, we found a new unforeseen low-energy structure after the

CASSCF relaxation, namely the singlet PBPb. This might give a clue that a new low-energy isomer is waiting to be found. Even though the quest for the optimal structure of Na_{13}^{+} began back in 1984, perhaps there are some unknown isomers that are energetically favorable for this 13 atom cluster.

Conclusions

Twelve isomers of the three lowest spin states of the Na_{13}^{+} cluster have been studied using hybrid DFT (PBE0, B3LYP and M06-2X XC functionals) and benchmark multireference CASSCF(12,12) + CASPT2(12,12) computations with a couple of Dunning's correlation consistent basis set. The optimized geometries and energetics have been reported. The following conclusions arise from the results.

The hybrid XC functional optimized geometries differ considerably from the geometries optimized with the CASSCF(12,12) method, thus showing the crucial role played by the non-dynamical correlation effects neglected in all the previous DFT studies of this cluster. For instance, the CSAP-(2,2) triplet is unstable at the CASSCF(12,12)/cc-pVDZ level and deforms into PBPa. Furthermore, both the C1-Solov and the GCL CASSCF(12,12)/cc-pVDZ optimized structures get quite distorted as compared with the PBE0, B3LYP and M06-2X optimized geometries.

Of particular importance is the fact that the relative energies of all isomers differ considerably between the hybrid DFT and CASSCF-CASPT2 methods. However, this can be explained since Kohn-Sham DFT is a single-reference approach and the CASSCF wavefunctions for all isomers and spin states show a rather large multireference character. This confirms, once again, the importance of the non-dynamical electron correlation effects in these alkali-metal clusters, making only large multireference wavefunctions reasonable as a zeroth-order reference for further treatment of the dynamic electron correlation.

We found a new and unexpected lowest energy isomer with the CASSCF(12,12)+ CASPT2

approach, i.e. the PBPb singlet.

The present CASSCF+CASPT2 results provide benchmark structural and energetic properties for the lowest three spin multiplicities. Our CASPT2 relative energies reveal several quasi-degenerate but topologically different isomers, even with different spin multiplicities. This suggest a strong dynamical behavior of Na_{13}^+ at finite temperature.

The adiabatic ionization energy of the neutral cluster computed both with PBE0/cc-pVTZ and the CASPT2/cc-pVDZ approach are in excellent agreement with the experimental figure (3.6 eV). However, we have explicitly shown that the good agreement obtained with the hybrid Kohn-Sham approach arises due to a lucky cancellation of errors given the rather strong multireference character of the wavefunctions, which lead to very different optimal geometries when the CASSCF(12,12)+CASPT2 method is applied.

Prediction of lowest energy structures and electronic properties are found to be crucially dependent on both, the non-dynamical and dynamical electronic correlation treatment.

ORCID

Emiliano Isaías Alanís-Manzano: orcid.org/0000-0003-4638-1091

Alejandro Ramírez-Solís: orcid.org/0000-0002-8428-5714

References

(1) De Heer, W. A. The physics of simple metal clusters: experimental aspects and simple models. *Reviews of Modern Physics* **1993**, *65*, 611.

(2) Reinhard, P.-G.; Suraud, E. *Introduction to cluster dynamics*; John Wiley & Sons, 2008.

(3) Dinh, P. M.; Reinhard, P.-G.; Suraud, E. *An introduction to cluster science*; John Wiley & Sons, 2013.

(4) Cohen, M.; Tielens, A.; Bregman, J. Mid-infrared spectra of WC 9 stars-The composition of circumstellar and interstellar dust. *The Astrophysical Journal* **1989**, *344*, L13–L16.

(5) Kroto, H. W. The chemistry of the interstellar medium. *Philosophical Transactions of the Royal Society of London. Series A, Mathematical and Physical Sciences* **1988**, *325*, 405–421.

(6) Weltner Jr, W.; Van Zee, R. J. Carbon molecules, ions, and clusters. *Chemical Reviews* **1989**, *89*, 1713–1747.

(7) Saykally, R. J. A search for pure carbon clusters in the ISM. *California Univ., Berkeley Report* **1994**,

(8) Eberhardt, W. Clusters as new materials. *Surface Science* **2002**, *500*, 242–270.

(9) Castleman Jr, A.; Khanna, S. Clusters, superatoms, and building blocks of new materials. *The Journal of Physical Chemistry C* **2009**, *113*, 2664–2675.

(10) Bhattacharyya, K.; Mukherjee, S. Fluorescent metal nano-clusters as next generation fluorescent probes for cell imaging and drug delivery. *Bulletin of the Chemical Society of Japan* **2018**, *91*, 447–454.

(11) Dong, F.; Guo, W.; Bae, J.-H.; Kim, S.-H.; Ha, C.-S. Highly Porous, Water-Soluble, Superparamagnetic, and Biocompatible Magnetite Nanocrystal Clusters for Targeted Drug Delivery. *Chemistry–A European Journal* **2011**, *17*, 12802–12808.

(12) Muetterties, E. L. Molecular metal clusters as catalysts. *Catalysis Reviews—Science and Engineering* **1981**, *23*, 69–87.

(13) Muetterties, E. L.; Krause, M. J. Catalysis by molecular metal clusters. *Angewandte Chemie International Edition in English* **1983**, *22*, 135–148.

(14) Martins, J. L.; Car, R.; Buttet, J. Electronic properties of alkali trimers. *The Journal of Chemical Physics* **1983**, *78*, 5646–5655.

(15) Pérez, J. F.; Florez, E.; Hadad, C. Z.; Fuentealba, P.; Restrepo, A. Stochastic search of the quantum conformational space of small lithium and bimetallic lithium- sodium clusters. *The Journal of Physical Chemistry A* **2008**, *112*, 5749–5755.

(16) Bonačić-Koutecký, V.; Pittner, J.; Fuchs, C.; Fantucci, P.; Guest, M.; Koutecký, J. Ab initio predictions of structural and optical response properties of Na_n^+ clusters: Interpretation of depletion spectra at low temperature. *The Journal of Chemical Physics* **1996**, *104*, 1427–1440.

(17) Zope, R. R.; Baruah, T.; Pederson, M. R. Polarizabilities of intermediate sized lithium clusters from density-functional theory. *Journal of Computational Methods in Sciences and Engineering* **2007**, *7*, 495–505.

(18) Knight, W.; De Heer, W. A.; Saunders, W. A.; Clemenger, K.; Chou, M.; Cohen, M. L. Alkali metal clusters and the jellium model. *Chemical Physics Letters* **1987**, *134*, 1–5.

(19) Pacchioni, G.; Beckmann, H.-O.; Koutecký, J. Investigation of alkali-metal clusters with pseudopotential multireference double-excitation configuration interaction method. *Chemical Physics Letters* **1982**, *87*, 151–158.

(20) Fantucci, P.; Koutecký, J.; Pacchioni, G. Calculated properties of alkali metal clusters with fivefold symmetry. *The Journal of Chemical Physics* **1984**, *80*, 325–328.

(21) Martins, J. L.; Buttet, J.; Car, R. Equilibrium geometries and electronic structures of small sodium clusters. *Physical Review Letters* **1984**, *53*, 655.

(22) Boustani, I.; Pewestorf, W.; Fantucci, P.; Bonaić-Koutecký, V.; Koutecký, J. Systematic ab initio configuration-interaction study of alkali-metal clusters: Relation between

electronic structure and geometry of small Li clusters. *Physical Review B* **1987**, *35*, 9437.

(23) Bonaić-Kouteckỳ, V.; Fantucci, P.; Kouteckỳ, J. Systematic ab initio configuration-interaction study of alkali-metal clusters. II. Relation between electronic structure and geometry of small sodium clusters. *Physical Review B* **1988**, *37*, 4369.

(24) Temelso, B.; Sherrill, C. D. High accuracy ab initio studies of Li_6^+, Li_6^-, and three isomers of Li_6. *The Journal of Chemical Physics* **2005**, *122*, 064315.

(25) Bonacic-Koutecky, V.; Fantucci, P.; Koutecky, J. Quantum chemistry of small clusters of elements of groups Ia, Ib, and IIa: fundamental concepts, predictions, and interpretation of experiments. *Chemical Reviews* **1991**, *91*, 1035–1108.

(26) Bonačič-Kouteckỳ, V.; Fantucci, P.; Kouteckỳ, J. An ab initio configuration interaction investigation of the excited states of the Li_4 cluster. *Chemical Physics letters* **1988**, *146*, 518–523.

(27) Kouteckỳ, J.; Boustani, I.; Bonačića-Kouteckỳ, V. Triplet-singlet splitting of the alkali metal clusters: Example of the Li_6 clusters. *International Journal of Quantum Chemistry* **1990**, *38*, 149–161.

(28) Bonačić-Kouteckỳ, V.; Fantucci, P.; Kouteckỳ, J. An ab initio configuration interaction study of the excited states of the Na_4 cluster: Assignment of the absorption spectrum. *Chemical Physics letters* **1990**, *166*, 32–38.

(29) Blanc, J.; Bonačić-Kouteckỳ, V.; Broyer, M.; Chevaleyre, J.; Dugourd, P.; Kouteckỳ, J.; Scheuch, C.; Wolf, J.; Wöste, L. Evolution of the electronic structure of lithium clusters between four and eight atoms. *The Journal of Chemical Physics* **1992**, *96*, 1793–1809.

(30) Żuchowski, P. S.; Hutson, J. M. Reactions of ultracold alkali-metal dimers. *Physical Review A* **2010**, *81*, 060703.

(31) Alanís-Manzano, E. I.; Ramírez-Solís, A. On the structure of the lowest spin states of Li_{13}^+. Hybrid DFT vs. benchmark CASSCF-CASPT2 studies. *Computational and Theoretical Chemistry* **2021**, *1200*, 113230.

(32) de Heer, W. A.; Knight, W.; Chou, M.; Cohen, M. L. Electronic shell structure and metal clusters. *Solid State Physics* **1987**, *40*, 93–181.

(33) Knight, W.; Clemenger, K.; de Heer, W. A.; Saunders, W. A.; Chou, M.; Cohen, M. L. Electronic shell structure and abundances of sodium clusters. *Physical Review Letters* **1984**, *52*, 2141.

(34) Brack, M. The physics of simple metal clusters: self-consistent jellium model and semi-classical approaches. *Reviews of Modern Physics* **1993**, *65*, 677.

(35) Reinhard, P.; Suraud, E. Metal Clusters, edited by W. Ekardt. 1999.

(36) Saito, Y.; Noda, T. *Small Particles and Inorganic Clusters*; Springer, 1989; pp 225–227.

(37) Martins, J. L.; Buttet, J.; Car, R. Electronic and structural properties of sodium clusters. *Physical Review B* **1985**, *31*, 1804.

(38) Iñiguez, M.; Lopez, M.; Alonso, J.; Soler, J. Electronic and atomic structure of Na, Mg, Al and Pb clusters. *Zeitschrift für Physik D Atoms, Molecules and Clusters* **1988**, *11*, 163–174.

(39) López, M.; Iñiguez, M.; Alonso, J. Stability of isomeric Na_n clusters. *Zeitschrift für Physik D Atoms, Molecules and Clusters* **1991**, *19*, 141–143.

(40) Calvo, F.; Tran, S.; Blundell, S.; Guet, C.; Spiegelmann, F. Three-dimensional global optimization of Na_n^+ sodium clusters in the range $n < \sim 40$. *Physical Review B* **2000**, *62*, 10394.

(41) Solov'yov, I. A.; Solov'yov, A. V.; Greiner, W. Structure and properties of small sodium clusters. *Physical Review A* **2002**, *65*, 053203.

(42) Hsing, C.; Ríos, P. L.; Needs, R.; Wei, C. Quantum Monte Carlo studies of 13-atom simple metallic clusters. *Physical Review B* **2013**, *88*, 165412.

(43) Poteau, R.; Spiegelmann, F. Structural properties of sodium microclusters (n= 4–34) using a Monte Carlo growth method. *The Journal of Chemical Physics* **1993**, *98*, 6540–6557.

(44) Frisch, M. J. et al. Gaussian 09 Revision C.01. Gaussian, Inc.: Wallingford, CT, 2009.

(45) Perdew, J. P.; Ernzerhof, M.; Burke, K. Rationale for mixing exact exchange with density functional approximations. *Journal of Chemical Physics* **1996**, *105*, 9982–9985.

(46) Becke, A. D. Density-functional exchange-energy approximation with correct asymptotic behavior. *Physical Review A* **1988**, *38*, 3098.

(47) Lee, C.; Yang, W.; Parr, R. G. Development of the Colle-Salvetti correlation-energy formula into a functional of the electron density. *Physical Review B* **1988**, *37*, 785.

(48) Vosko, S. H.; Wilk, L.; Nusair, M. Accurate spin-dependent electron liquid correlation energies for local spin density calculations: a critical analysis. *Canadian Journal of Physics* **1980**, *58*, 1200–1211.

(49) Zhao, Y.; Truhlar, D. G. The M06 suite of density functionals for main group thermochemistry, thermochemical kinetics, noncovalent interactions, excited states, and transition elements: two new functionals and systematic testing of four M06-class functionals and 12 other functionals. *Theoretical Chemistry Accounts* **2008**, *120*, 215–241.

(50) Francl, M. M.; Pietro, W. J.; Hehre, W. J.; Binkley, J. S.; Gordon, M. S.; DeFrees, D. J.; Pople, J. A. Self-consistent molecular orbital methods. XXIII. A polarization-type basis set for second-row elements. *J. Chem. Phys.* **1982**, *77*, 3654–3665.

(51) Dunning Jr, T. H. Gaussian basis sets for use in correlated molecular calculations. I.

The atoms boron through neon and hydrogen. *Journal of Chemical Physics* **1989**, *90*, 1007–1023.

(52) Werner, H.-J.; Knowles, P. J.; Knizia, G.; Manby, F. R.; Schütz, M. Molpro: a general-purpose quantum chemistry program package. *Wiley Interdisciplinary Reviews: Computational Molecular Science* **2012**, *2*, 242–253.

(53) Herrmann, A.; Schumacher, E.; Wöste, L. Preparation and photoionization potentials of molecules of sodium, potassium, and mixed atoms. *The Journal of Chemical Physics* **1978**, *68*, 2327–2336.

(54) Röthlisberger, U.; Andreoni, W. Structural and electronic properties of sodium microclusters (n= 2–20) at low and high temperatures: New insights from abinitio molecular dynamics studies. *The Journal of Chemical Physics* **1991**, *94*, 8129–8151.

(55) Röthlisberger, U.; Andreoni, W.; Giannozzi, P. Thirteen-atom clusters: Equilibrium geometries, structural transformations, and trends in Na, Mg, Al, and Si. *The Journal of Chemical Physics* **1992**, *96*, 1248–1256.

(56) Kronik, L.; Vasiliev, I.; Jain, M.; Chelikowsky, J. R. Ab initio structures and polarizabilities of sodium clusters. *The Journal of Chemical Physics* **2001**, *115*, 4322–4332.

(57) Huwig, K.; Grigoryan, V.; Springborg, M. Global optimization of Li and Na clusters: application of a modified embedded atom method. *Journal of Cluster Science* **2019**, 1–22 [and references therein].

(58) Chang, C.; Chou, M. Alternative low-symmetry structure for 13-atom metal clusters. *Physical review letters* **2004**, *93*, 133401.

Graphical TOC Entry

> Some journals require a graphical entry for the Table of Contents. This should be laid out "print ready" so that the sizing of the text is correct.
>
> Inside the `tocentry` environment, the font used is Helvetica 8 pt, as required by *Journal of the American Chemical Society*.
>
> The surrounding frame is 9 cm by 3.5 cm, which is the maximum permitted for *Journal of the American Chemical Society* graphical table of

content entries. The box will not resize if the content is too big: instead it will overflow the edge of the box.

This box and the associated title will always be printed on a separate page at the end of the document.